Automatic Craniofacial Structure Detection on Cephalometric Images

Tanmoy Mondal, Ashish Jain, and H. K. Sardana

***Abstract*—Anatomical structure tracing on cephalograms is a significant way to obtain cephalometric analysis. Cephalometric analysis is divided in two categories, manual and automatic approaches. The manual approach is limited in accuracy and repeatability due to differences in inter- and intra-personal marking. In this paper, we have attempted to develop and test a novel method for automatic localization of craniofacial structures based on the detected edges in the region of interest. Before edge detection of the particular region, the region was filtered by adaptive non local filter for noise removal by keeping the edge information undisturbed. According to the gray-scale feature at the different regions of the cephalograms, modified Canny edge detection algorithm for obtaining tissue contour was proposed. With the application of morphological opening and edge linking approaches, an improved bidirectional contour tracing methodology was proposed by an interactive selection of the starting edge pixels, the tracking process searches repetitively for an edge pixel at the neighborhood of previously searched edge pixel to segment images, and then craniofacial structures are obtained. The effectiveness of the algorithm is demonstrated by the preliminary experimental results obtained with the proposed method.**

***Index Terms*—Cephalograms, cephalometric analysis, contour tracing, craniofacial structure, image segmentation.**

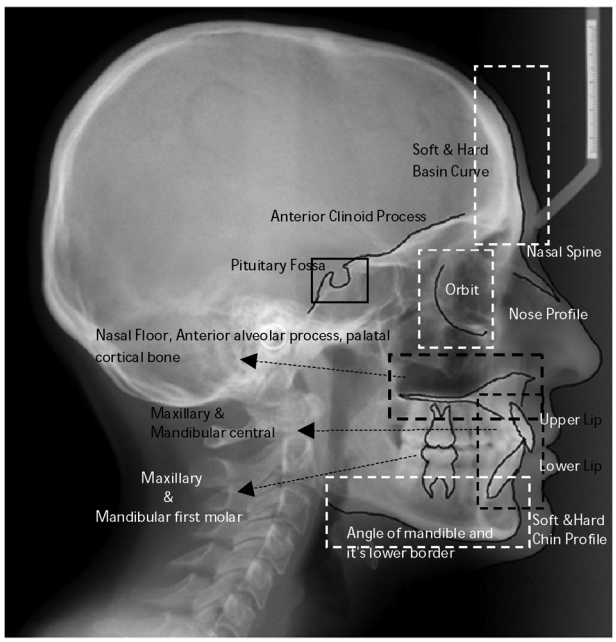

Fig. 1. Desired craniofacial structures required for cephalometric analysis.

I. Introduction

In cephalometric analysis, dentists are required to identify predefined characteristic anatomical landmarks and craniofacial structures on a cephalometric radiograph (X-ray head film) to diagnose cranial bone structures of their patients. The difficulty of identifying these landmarks is compounded by variability of patient's skull structure and nature of the radio-graph images, for which most dentists have to use their expertise gained through several years of clinical practice. Any competitive image recognition system has to match the accuracy close to Digital Object Identifier human performance, and thus stringent requirements on tolerance of location estimation are imposed. The conventional method of locating cranial bone structures depend on manual tracing of the radiograph images. Fig. 1 demonstrates all of the required cranial bone structures for cephalometric analysis; the names of the specific structures are denoted along with the structure.

Here, the research advancement in the field of automatic detection of craniofacial structures has been portrayed. Hutton *et al.* [1] used the active shape model (ASM), originally explained by Cootes *et al.* [2], [3] for tracing craniofacial structures on cephalometric images. Permissible deformation of a template was established from a training set of hand-annotated images and the resulting model was used to fit in the unseen images. ASM required a training set of hand-annotated images. The annotation took the form of a set of points joined with line segments, which is a representation generated by outlining the major structures in the image. They used 63 randomly selected cephalogram images and tested the training set with "drop one out" method and reported that 13% of 16 landmarks were within ± 1 mm, 35% within ± 2 mm, and 74% within ± 5 mm. The authors concluded that ASM did not give sufficient accuracy for landmark detection in clinical applications and could only be used as a good starting point for global landmark identification. Based on their given conclusion, Yue *et al.* [4] performed some modification on the original ASM as well as the shape variation modelling. By dividing each training image into several structures based on independent regions and using these regions

Manuscript received June 20, 2010; revised January 11, 2011; accepted March 02, 2011. Date of publication March 24, 2011; date of current version August 19, 2011. This work was supported by the Council of Scientific & Industrial Research (CSIR), India, under Grant SIP-022.08. The associate editor coordinating the review of this manuscript and approving it for publication was Dr. Patrick Flynn.

T. Mondal was with Computational Instrumentation Unit, Central Scientific Instruments Organisation (CSIO), Chandigarh, 160030, India. He is now with Graphics and Intelligence Based Script Technology, Centre for Development of Advanced Computing, Pune, India (e-mail: tanmoy.besu@gmail.com).

A. Jain and H. K. Sardana are with the Computational Instrumentation Unit, Central Scientific Instruments Organisation (CSIO), Chandigarh, India (e-mail: hk_sardana@csio.res.in).

Color versions of one or more of the figures in this paper are available online at http://ieeexplore.ieee.org.

Digital Object Identifier 10.1109/TIP.2011.2131662

as the basic of shape modeling and feature point localization, landmarks are detected. Craniofacial structures are traced by four point subdivision schemes in their work. Rueda and Alcaniz [5] used active appearance model (AAM), which contains a statistical model of shape and gray-level appearance of an object of interest and represents both shape and texture variations of the region covered by the model. AAM model was used for localization of a considerable amount of landmarks. In this research, top-hat transformation was used to correct the intensity in homogeneity of the radiograph, generating a consistent training set. They reported an average accuracy of 2.48 mm, when the AAM model trained by 96 hand-annotated images and tested with a "drop one out" method. This is merely the same approach described by Saad *et al.* [6]: their paper describes AAM and simulated annealing for automatic cephalometric analysis. A comparison of the results showed 25% accuracy improvement over ASM. Vucinic *et al.* [7] demonstrated automatic land-marking of cephalometric images using AAMs. Multiresolution implementation was used, in which AAM was iterated to convergence at each level before projecting the current solution to the next level of the model. Sixty randomly selected images was used for training and tested with a leave-five-out method, which resulted in an average accuracy of 1.68 mm, with 61% of landmarks detected within 2 mm and 95% landmarks detected within 5 mm of precision.

To our knowledge, the last few years have witnessed major advancements in precision-based landmark detection, but less has been reported on detection of craniofacial structures on cephalometric images. Most of the methodologies have been based on tailored-made model-based approaches (i.e., ASM and AAM). As the described approaches were fitting a predescribed model to the tested image, in case of ASM, where the search is made around the current position of each point using a model of the image texture in small regions around each feature points, the AAM manipulates a full model of appearance, which represents both shape variation and texture of the region covered by the model. AAM is used to generate full synthetic images of the model objects; it then uses the difference between the current synthesized image and target image to update the parameters of all the required structures but failed in terms of precision and accuracy.

From the prior knowledge of cephalometric analysis as observed from our work, we can study some of the following facts: 1) prior knowledge is essential in structure detection and 2) knowledge of intensities at different portions of the structure is required for defining the threshold values in a Canny edge detection algorithm. In this paper, we have proposed a modified edge detection approach for detecting the craniofacial structures of cephalograms; this algorithm contributes in the aspects given here.

- A significant method for template matching, a knowledge-based template is selected, and pattern matching approach is used for detecting the location of our desired structure.
- Adaptive nonlocal filtering is applied at the detected portion for denoising the image.
- Edge detection methodology is performed on the filtered images. For edge detection, an inimitable procedure is applied by the modification of the original Canny edge detection algorithm.
- Morphological opening, i.e., repeated dilation and erosion are applied for linking the broken edges.
- Next, a local edge linking approach is applied for connecting the broken edges in the edge maps.
- Thereafter, tracking of desired edge from the edge maps is done and subsequently plotting them onto the whole image is done to get the desired structures.

The remainder of this paper is organized as follows. The contribution is depicted in Section II, in which we show how the new method is suitable for extracting most of the craniofacial structure required for cephalometric analysis. In Section III, by describing the result and discussion, it is apparent how the approach is efficient for fulfilling the requirement.

II. Materials and Methods

A. Material

The cephalometric images were randomly selected without any judgement of their quality, sex, and age to ascertain that the proposed methodologies are free from any form of bias to obtain the desired results. In this research, 85 pretreatment cephalograms were used. In this full dataset, a set of 30 digital images in DICOM format of 300 dpi $(1 \text{ pixel} = 0.084 \text{ mm})$ resolution (dataset1), and 2400 $\times$ 3000 pixels, were obtained by scanning the X-ray films with a "VIDAR VXR-12" scanner. Another set of 55 digital images (referred to as dataset2) were obtained by "Strato 2000 Full Digital Dental Panoramic System" with a resolution of 194 dpi $(1 \text{ pixel} = 0.14 \text{ mm})$ and with a size of 1537 $\times$ 1171 pixels in JPEG format.

B. Methods

1) Region Detection: As the first step of the proposed algorithm, we have applied an effective template matching approach to determine the location of our desired craniofacial structures. In this work, the search was performed by 2-D normalized cross correlation [8] between the predefined search area in the image and the predefined template, thus finding the position with highest correlation value in the image. The major limitation of above method is high computational cost associated with large window size of search area in desired image and inability of resisting image distortion. To minimize the processing time and eliminate the risk of false detection due to image distortion, an efficient pattern-matching approach was applied only in the zones determined by a prior knowledge of human skull, i.e., as the location of each requisite region of interest is known from the prior knowledge of human skull, e.g., the location of the tripod rod always belongs to the first quadrant of the image, so we search for this specific template in the given specific region only. In general, for detecting each region of interest separately, first this fixed tripod rod, which is common in every image, is detected. Defining the location of the rod as an entry region of the image, based on the located area of the rod in the image, at first the required nose region was detected. As from the detection of the tripod rod, we can estimate the most probable range of the region in which the desired nose region can be located, thus, for less computational expensiveness, pattern-matching approaches are applied in this specific range of region only. After locating the nose region

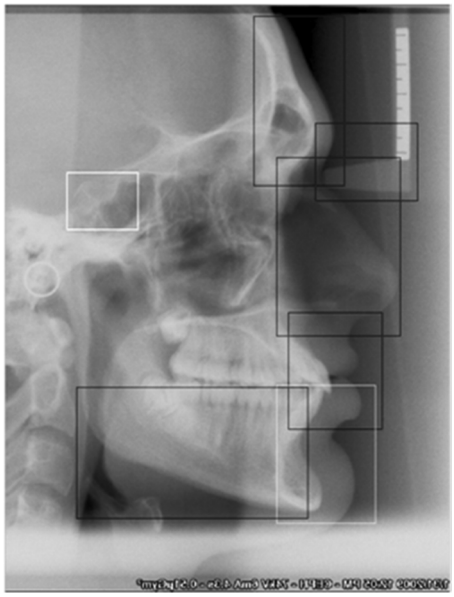

Fig. 2. Results of region detection by template matching approach.

based on the noise location, the lip region is detected in the same manner. For detecting next undetected region of interest, the previously located region nearest to this undetected region is always considered. By proceeding in this manner all the remaining regions of interest were detected. Fig. 2 shows the results of detection of desired regions.

2) Adaptive Nonlocal Filtering: After region detection, adaptive nonlocal filtering is performed on each region of interest. However, anisotropic diffusion happens in homogeneous areas and along edges, but stops when it encounters object contour. It then adaptively produces sharp boundaries of smooth regions. By adjusting parameters of the diffusion model, we could yield images in different scales. Perona and Malik [9] suggested a diffusion model, which is computationally expensive because of its higher iterative nature. Filtering with a kernel that is symmetric around the center pixel results in averaging of edge values and hence blurring of the edges. In order to alleviate this problem, Nitzberg and Shiota [10] proposed an offset term which pushes the center of the kernel from the point to be filtered. The main purpose of this type of offset vector field is to displace the filters away from the border areas to preserve the edge information at the border area. Fischl and Schwartz [11] proposed this displacement in the direction normal to the boundary of a region, as this is the direction with no component of edge. Fischl and Schwartz. proposed a fast realization, in which serial diffusion is replaced with parallel kernel operations performed in a single step. For each located region, the adaptive nonlocal filtering proposed by Fischl and Schwartz is used to reduce noise in the selected ROI. With parallel diffusion, features at various scales are filtered nonlocally at the offset positions using the kernel of different sizes. In this filtering approach, the relation between the scale and distance is made explicit via the magnitude of the displacement vector at a given location. Large offset relates to a longer displacement vector, which is useful for locating the contour of large structures, whereas a minuend structure is associated with a small scale and small magnitude of displacement vector. Smoothing associated with the filtering process may be accomplished using standard fixed size filters. This filtering approach denoises the image without disturbing the edge information, so after filtering operation edge detection approach has been introduced.

3) Modification of Canny's Edge Detection Algorithm: After performing the filtering operation on the selected region, the edges in the region of the image are detected by Canny edge detector. In this method, the image is first smoothened by Gaussian filter to reduce noise in the image, and then spatial gradient calculation is performed by the Gaussian kernel so that gradient magnitude Gx for horizontal direction and Gy for vertical direction for each pixel can be measured. The edge direction of every pixel can be measured by $\theta = arc\ tan(Gy/Gx)$. Nonmaximum suppression in the edge direction is performed, which suppress any pixel whose gradient magnitude is not at maximum, this nonmaximum suppression gives a thin edge in the later processed image. Furthermore, a suitable pair of threshold values is selected to track the remaining pixels that have not been suppressed to eliminate streaking. The higher threshold value (HTV) is automatically selected according to the histogram and the lower threshold value (LTV) is then calculated as $0.4 \times$ HTV; however, it is difficult to automatically select a suitable pair of HTV and standard deviation (SD) for detecting a soft tissue profile as well as a hard tissue profile in a set of cephalometric images due to the local intensity variability and low contrast of the hard tissue profile against the soft tissue, but the methodology described above is helpful for selecting threshold values.

After selecting the threshold values, verification was performed using LTV and HTV values against those pixels, respectively, which were returned by the nonmaximal suppression operation as follows.

- If the gradient at that pixel is greater than HTV, then the pixel is chosen as an edge pixel.
- If the gradient at the pixel is below the LTV then, the pixel is declared as a "nonedge pixel."
- If the gradient of the edge pixel is between the LTV and the HTV, then it is declared as an "edge pixel" if and only if it is connected to an edge pixel directly or via the pixels between the LTV and HTV.

For the edge detection, the selection of both LTV and HTV can be made empirically by experiments. By inspecting the output of the edge detection, a suitable pair of LTV and HTV can be selected. This HTV and LTV pair is used for detecting not only the large edges but also the small edges within the entire image. Due to the local intensity variability and low contrast of the small desired curves against the background, the original Canny edge detector failed to detect some of desired edge, so modification of canny edge detection technique proposed by Chang and Gong [12] have been applied. The modified Canny edge detection algorithm was developed to determine the HTV and LTV based on the local connection of any selected edge point. The algorithm is given here.

Step 1) The edge points detected by Canny edge detection algorithm, the location of the candidate points, and the magnitude of the entire pixel are selected.

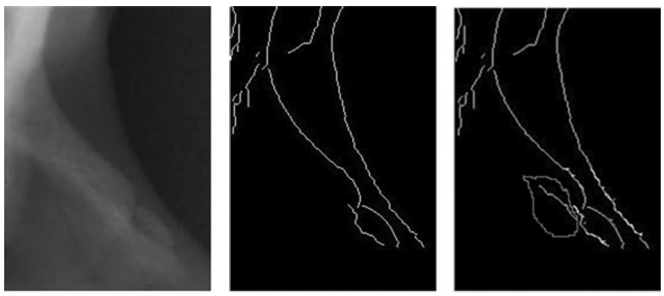

(a) (b) (c)

Fig. 3. (a) Original image. (b) Edge detected by Canny edge detector. (c) Portion enclosed is the edge detected by modified Canny's edge detection algorithm.

Step 2) The Eigen value map of the image is generated this way.
  a) An ROI is selected which covers the structure of our interest.
  b) The Eigen value of a pixel is the minimum Eigen value of the matrix of the neighborhood centred at the pixel.

Step 3) A threshold value of the Eigen value map is selected as the $(\text{maximum} + \text{minimum})/2$ of the Eigen value matrix.

Step 4) For any pixel with its corresponding Eigen value less than the threshold value, if its neighborhood contains a candidate point and an edge point crosses the pixel, i.e., the candidate point, the center pixel for which the neighborhood is formed and the edge point will lie in a straight line, then the gradient of the candidate point is selected as local dynamic HTV.

Step 5) Select new edge points in this locality using the local dynamic HTV and the global LTV.

By repetitive searching for new edge pixels in the selected region based on the created neighborhood centring the pixel of interest, the modified Canny edge detector results in some added edge pixels, The edge pixels by modified Canny edge detection operation are combined with the previously obtained edge pixels which were generated by normal Canny edge detection operation. Fig. 3 shows the application of the algorithm. Finally, the edge information is applied into the next module of the proposed methodology.

4) Edge Linking: After the previous module has converged, edge linking [13] is performed for joining the broken edge points. The basic idea is to use two edge images that have undergone hysteresis: a high image (obtained by a applying high threshold value so that only strong edges can be observed) and a low image (obtained by applying low threshold value so that weak as well as strong edge both can be observed). The main idea is to use the high image as guidance for promoting edges from the low image i.e., expressing them in the output image, so output image will consist of edges from high images and those edges which are promoted from the low image. The criterion for promotion of the edges from the low image is connectivity, whether the end points of the strong edges in the high image are connected by the weak edge points in the low image. The algorithm is given here.

Step 1) Subtract the edge points extracted by low image from the edge points extracted from high image, so that it forms a difference image.

Step 2) Determine the location of end points (refer to the Appendix) in the high image. Mark that location as the edge point in the difference image. After that, a neighborhood is formed centering the location of this edge points in the difference image.

Step 3) Now, for each such edge point in the difference image, we search the neighborhood for any of them as edge pixel and whether it connects to another end point in the high image.

Step 4) If a connection is discovered, then this traced edge in the difference image is qualified for addition in the final result, i.e., this edge is added with the edge information generated in the high image.

Fig. 4 demonstrates the outcome of the proposed methodology. For this strategy to be effective, there must be a significant difference in the thresholds used for the high and low images. However, selecting the HTV and LTV is a very critical job. In addition, edge linking also creates some unwanted branches of the edge which can be eliminated in the later stage by tracking the specified edge.

A repeated dilation and erosion has been introduced on the results obtained from the edge linking step to obtain better results. Fig. 5 demonstrates the outcome of the procedure.

5) Edge Tracking Module: After the above-mentioned module has converged, thereafter a novel bidirectional edge tracking approach [14] has been introduced for extracting the desired edges from the pool of edges. The aforementioned algorithm begins with choosing an edge point as the starting point from the pool of edges. Suppose the binary image matrix is M, the coordinate of the first edge point is $(\mathrm{x}_0, \mathrm{y}_0)$, and the next edge point must be located in its eight neighborhoods of it. In our proposed algorithm, we have applied a bidirectional mode contour tracing approach followed by tracking the edges in both directions one after another. Ascertaining the initial point as M, we perform a raster scan in the image until the first white pixel was not found. The confirmation of **edgelist {i}** is essential as **edgelist {i}** is a 2-D matrix having the coordinates of the edge pixels. We can determine the next edge point in **edgelist {i}** as our next edge point must be located in the neighborhood, i.e., at the locations 2, 4, 6, 8 or 1, 3, 5, 7 of our earlier selected edge pixel. Thus, neighborhood pixels were created around earlier selected edge pixels and were checked for their possibility of being a gray pixel. Whenever the gray edge pixels were detected, their locations were stored. Details are given below.

The edge tracking algorithm [15] is given by the following steps.

Step 1) As we track the edges on the binary image, so, the binary image have been used as an input to the tracking algorithm.

Step 2) The isolated pixels (a pixel surrounded by dark pixels) are removed from the image.

Step 3) Thinning operations [16] are performed on the binary image.

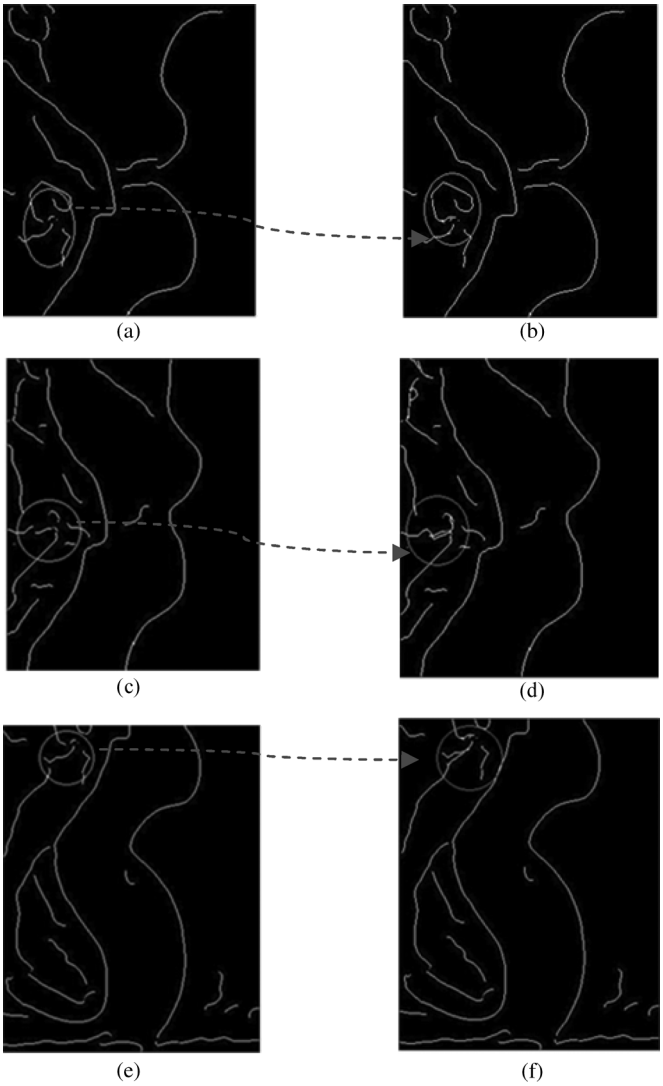

Fig. 4. Edge linking algorithm. (a), (c), (e) Encircled portion highlights, prior to the application of edge linking at different ROIs. (b), (d), and (f) Postapplication results of the algorithm.

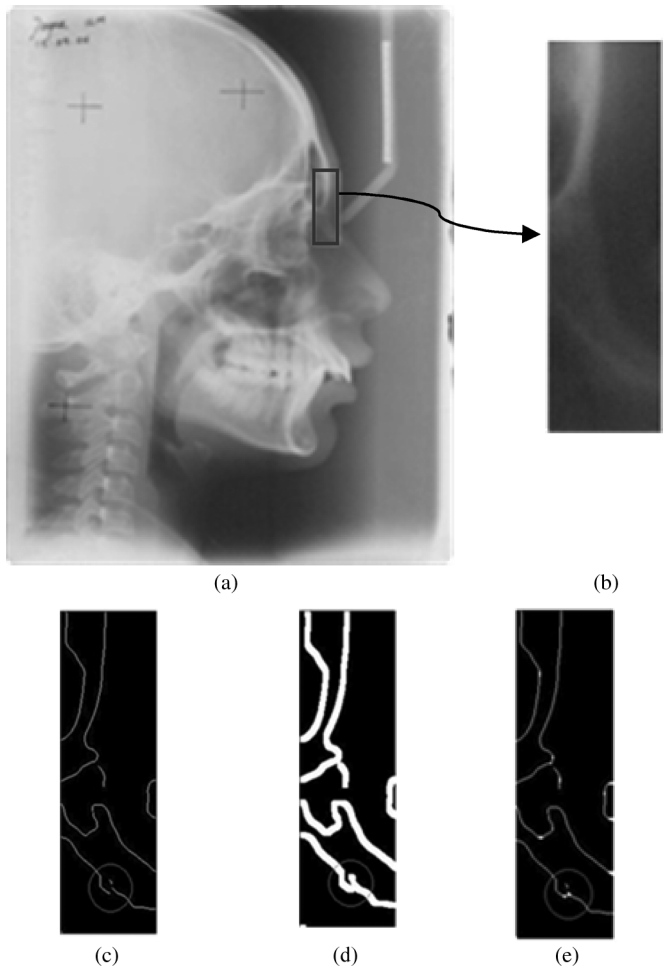

Fig. 5. (a) Enclosed portion shows the ROI. (b) Cropped portion of the image. (c) Edge detection on (b): the encircled portion shows broken edges caused due to edge detection. (d) Shown in the encircled portion, the broken edges are linked after repeated dilation. (e) As shown in the encircled portion, after a repeated number of dilation operations equaling the number of erosion operation, original binary image returns with linked broken edges.

Step 4) Perform a raster scan in the image until the edge pixel is not detected. Let the coordinate of the first edge pixel be (rstart, cstart). Make M $(\mathrm{rstart}, \mathrm{cstart}) = -\mathrm{curvno}$ (where curvno is a variable initialized to zero).

Step 5) Pixels surrounding this pixel is searched to locate the presence of any other white pixel $(\mathrm{value} = 1)$, if the white pixel is located, then it is accepted as a part of earlier detected edge and marked it as a collected point (to avoid repetition) and then proceeds to step 6). If the white pixel does not exist, go back to step 4).

Step 6) Pixels surrounding the previously determined pixel in step 5) is searched [say, (p,q)] and checked whether there is any other edge pixel [say, (s,r) whose $\mathrm{value} = 1$] in its neighborhood. If the white pixel exits, pick this edge point as the part of the current edge and mark it as a collected edge point, (i.e., make M $(\mathrm{s}, \mathrm{r}) = -\mathrm{curvno}$) if the following condition is satisfied.

- If this edge point [say (p,q)] itself has less than two neighboring pixels (i.e., two white pixels) connected back to our current edge, (i.e., which is not marked as collected edge point), then this step repeated, [go back to step 6)] until end of the edge. If it does not exist, proceed to step 7).

Step 7) Now, repeat the same step for tracking in the opposite direction from the location (rstart, cstart), i.e., go back to step 6).

Step 8) Make $\mathrm{curvno} = \mathrm{curvno} + 1$, perform the raster scan in the image until the untraced white pixel is not obtained, and let the location of the pixel be (rstart, cstart). Go to back step 6).

Continue in this manner until all of the edge points are traced. For removing the unwanted edges of shorter length, we have defined a constraint on the length of the collected edge. Then, by knowing the geometrical definition of the location and having the previous knowledge about the structure to be extracted, the edges are removed, if the length of the collected edge is not greater than the certain length defined by user. Those edges that are greater than or equal to that of the user-defined length, these

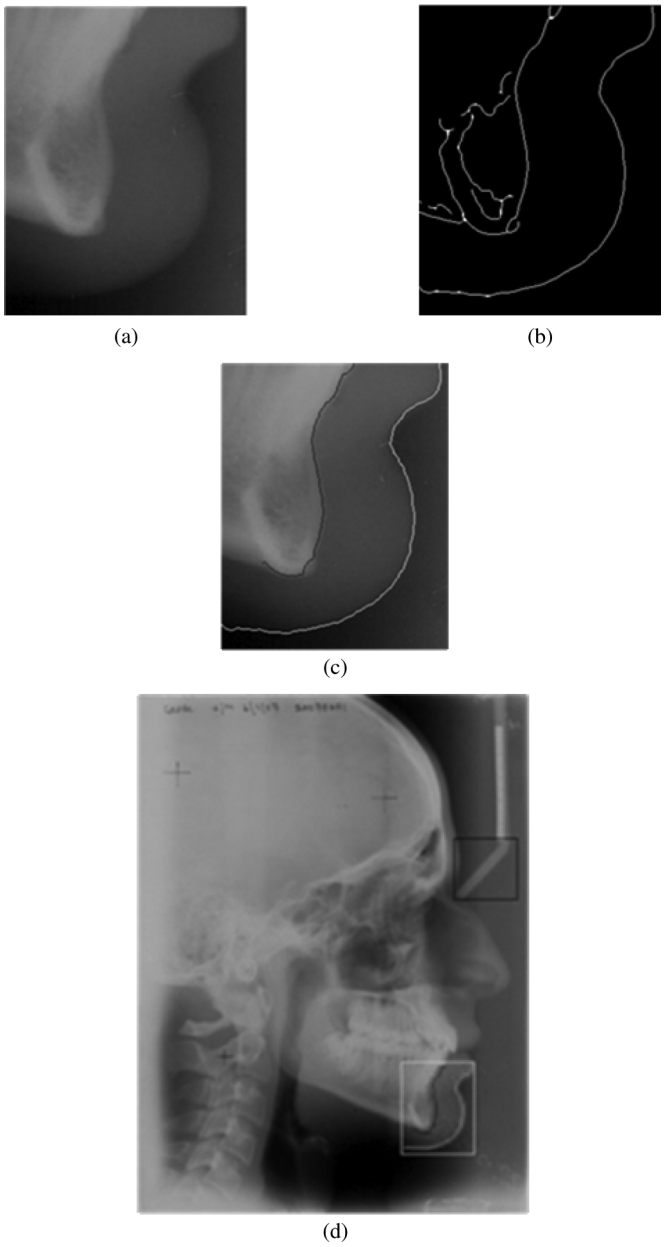

Fig. 6. (a) Template extracted from the main image. (b) Result of edge detection on cropped image. (c) Edge map on (a). (d) Edge map on the full image.

edges will qualify as the desired edge. Now, the edge points are extracted, and then the edge points are plotted on the original image. Fig. 6 demonstrates the outcome of the methodology.

III. Results and Discussion

1) Results: We applied our experiment in two sets of images, and results obtained by the algorithm were compared with those obtained by the human experts. By the observation of the application of this algorithm on dataset1 and dataset2 and considering a limit, if the particular structure is detected more than 80% of the required detection length of the structure, then that detection is considered as an acceptable detection. When the algorithm was tested on dataset1, the results revealed that the hard tissue profile of chin is detected in almost every image, and the soft tissue profile of the chin was detected in 83%–85% cases.

TABLE I
Success Rate of the Algorithm When Applied in Dataset 1 and Dataset 2

Name of the curve	Success Rate	
	Dataset1	Dataset2
Soft tissue profile of chin	83.34%	100%
Hard tissue profile of chin	96%	98%
Angle of mandible and it's lower border	90%	89%
Lower lip	93.34%	100%
Upper Lip	86.67%	100%
Soft nose tissue profile	73.34%	94.54%
Nasion	76.67%	90.91%
Soft basin curve	93.34%	100%
Hard basin curve	96.67%	100%
Pituitary Fossa	93.34%	87.27%

The angle of the mandible and its lower border was detected in 21 images but, in the remaining nine cases, the structure was partially detected; among those, six cases were acceptable as the detected length crossed the above-mentioned threshold value. Table I illustrates the success rate of this particular structure. Similarly, the portion of the lower lip was detected in 28 images, and this particular craniofacial structure failed detection in the remaining two images, whereas the upper lip was detected in 26 images and failed detection on the remaining four images. In the case of detection of a soft tissue nose profile, the experimental results shows that this structure was detected in 22 images, but, in the remaining eight cases, the proposed methodology failed to detect the specific structure. Table I illustrates this as well. The nasion curve was detected in 23 cases, and, in the remaining seven cases, the specific structure was not detected. Soft basin curve and hard basin curve were detected in most of the cases, but the pituitary fossa could not be detected. This may be attributed to a probable reason that the common threshold of the Canny algorithm does not work for all of the images as this is an ambiguous region. The algorithm was able to locate the structure impeccably in 26 cases, but in the remaining four cases it was not detected, Table I illustrates the aforementioned results.

On the second dataset, results show that the detection of the hard and soft tissue profiles of chin succeeded in almost every image. The angle of the mandible and its lower border was detected in 49 images but, in the remaining six cases, it failed to detect the structure. The upper lip and lower lip were detected in almost every image. Soft tissue nose profile was detected in 52 images, but in the remaining three cases the profile was not detected. The nasion curve was successfully detected in 50 cases. Soft basin curve and hard basin curve were detected in most of the cases, with a success rate of 98%. Pituitary fossa was detected by the algorithm in 48 cases, but only partially detected in the remaining seven cases. detected. Table I illustrates the success rate for each of the desired curves. Figs. 7, 8 reveal the results, as evaluated by the new algorithm. In this experiment, we also studied the effect of image source on detection results.

It was observed that images from two different sources did not affect the detection rate.

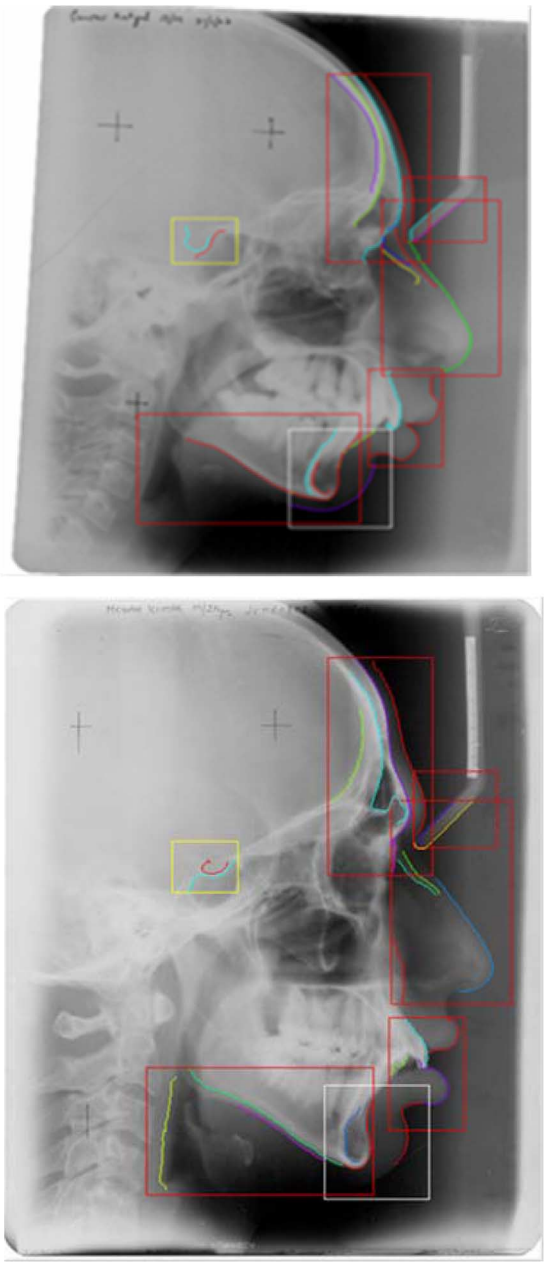

Fig. 7. Results of the proposed algorithm on dataset1.

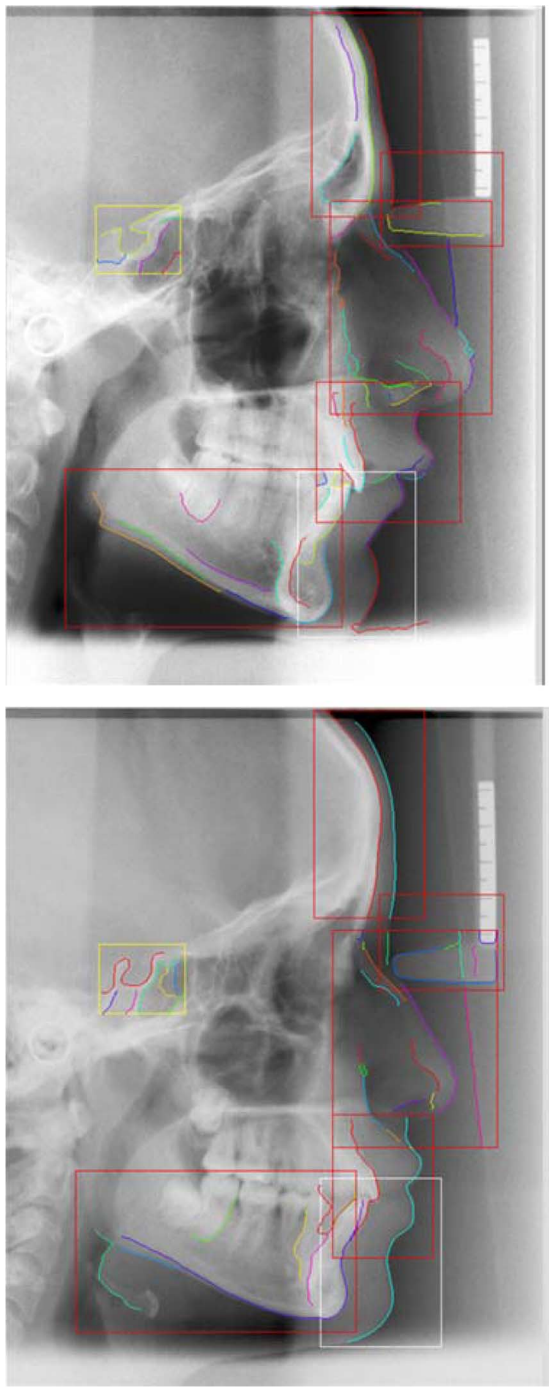

Fig. 8. Results of the proposed algorithm on dataset2.

As reviewed, not much has been explored regarding the accuracy of the detection of the craniofacial structures and curves. The majority of previous research has used the model-based approach and discussed the accuracy of the detection of the significant landmarks.

Hence, it becomes difficult to make a comparative study with earlier published results of accuracy of detection, as to the best of our knowledge there is hardly any literature depicting the accuracy of structure detection.

2) Discussion: Our work proposes a novel approach for detection of the craniofacial structures from cephalogram images. As it is based on the true edge detection in the image, it is susceptible to lower error range, though the major problem is the localization of the desired structures in the images, which is the existing problem with the template matching approach in medical images of lower quality, henceforth affecting rest of the results. As in the template matching approach, we find out the correlation at each pixel to fit the best place, with an increase in the image size, computation time increases. The proposed algorithm for edge linking and modification to the Canny edge detection method provides better result outcome wherein existing edge detection algorithms have limitations in result outcome with breaks in edge detected, our algorithm can overcome the aforementioned limitation. As the edge tracking algorithm depends upon the manually defined length of the desired curve,

the algorithm detects other undesirable edges of length greater than or equal to the defined length from the ROI, but those detected edges can be easily ignored during visual discernment by the doctor, so as observed from the experimental result that it is somewhat dependent on image parameters, it is also observed from the experimental result that all of the desired structures could not be detected by this proposed methodology, as structures like "anterior clinoid process," "nasal floor, anterior alveolar process, palatal cortical bone," and "orbit" are located at areas with higher radio opacity, so it is difficult to locate those particular structures. The structures named "maxillary and mandibular central and maxillary and Mandibular first molar" is a kind of predefined model, which is manually fitted by the skilled doctors at its plausible location. So to locate this particular structure, some model-based approaches like ASM or AAM can be attempted.

3) Conclusion and Future Work: The algorithm for the automated detection of craniofacial structures on 2-D cephalogram images was developed in this work. The anatomical structure extractions were obtained in a homogeneous framework for the first time. Our approach comprises image processing and pattern matching techniques for locating the ROI so that the desired craniofacial shape can be partitioned to some structure-based regions. The initial results show the advantage and reliability of the algorithm. Future endeavours would concentrate on bringing better results through larger datasets for clinical acceptance.

APPENDIX
POINT CLASSIFICATION

This method requires point classification as an initial step. Its purpose is to classify each pixel as one of the three types: end points, edge points, and intersection points. This is done by setting up a lookup table for finding end points and intersection points among the edge points. All possible 3×3 neighborhoods of the total edge image are created, and a check is performed whether the center pixel within the 3×3 neighborhood is an end point or a junction point. This is done by creating a constraint that to be checked for end point or intersection point. The constraint is that the center pixel must be set (1) and the number of transitions/crossing between 0 and 1 as one traverses the perimeter of the 3×3 region must be 6 or 8 for an intersection point and 2 for an end point.

ACKNOWLEDGMENT

The authors would like to thank the Post Graduate Institute of Medical Research, Chandigarh and Centre for Dental Education and Research, All India Institute of Medical Science, New Delhi, India, for their contribution and for providing the cephalometric image database. The authors would also like to thank the anonymous reviewers, Prof. P. Flynn, Dr Viren Sardana and Mr Prasoon Kumar, whose suggestions significantly improved the original manuscript.

REFERENCES

[1] T. J. Hutton, S. Cunningham, and P. Hammond, "An evaluation of active shape models for the automatic identification of cephalometric landmarks," *Trans. Eur. J. Orthodont.*, vol. 22, no. 5, pp. 499–508, 2000.

[2] T. F. Cootes, C. J. Taylor, D. H. Cooper, and J. Graham, "Active shape models—Their training and application," *J. Comput. Vis. Image Understanding*, vol. 61, no. 1, pp. 38–59, Jan. 1995.

[3] T. F. Cootes, C. J. Taylor, D. H. Cooper, and J. Graham, "Training models of shape from sets of examples," in *Proc. Brit. Mach. Vis. Conf.*, 1992, pp. 9–18.

[4] W. Yue, D. Yin, C. Li, G. Wang, and T. Xu, "Automated 2-D cephalometric analysis on X-ray images by a model-based approach," *IEEE Trans. Biomed. Eng.*, vol. 53, no. 8, pp. 1615–1623, Aug. 2000.

[5] S. Rueda and M. Alcaniz, "An approach for the automatic cephalometric landmark detection using mathematical morphology and active appearance models," in *Proc. Med. Image Comput. Assisted Intervention*, 2006, vol. 4190, no. 2006, pp. 159–166.

[6] A. A. Saad, A. El-Bialy, A. H. Kandil, and A. S. Ahmed, "Automatic cephalometric analysis using active appearance model and simulated annealing," in *Proc GVIP Conf.*, Dec. 2005, vol. 6, pp. 19–21.

[7] P. Vucinic, Z. Trpovski, and I. Scepan, "Automatic landmarking of cephalograms using active appearance models," *Eur. J. Orthodont.*, vol. 32, no. 3, pp. 233–241, Mar. 4, 2010.

[8] L. Di Stefano, S. Mattoccia, and M. Mola, "An efficient algorithm for exhaustive template matching based on normalized cross correlation," in *Proc. 12th IEEE Int. Conf. Image Anal. Processi.*, Sep. 29, 2003, pp. 322–327.

[9] P. Perona and J. Malik, "Scale space and edge-detection using anisotropic diffusion," *IEEE Trans. Pattern Anal. Mach. Intell.*, vol. 12, no. 7, pp. 629–639, Jul. 1990.

[10] M. Nitzberg and T. Shiota, "Nonlinear image filtering with edge and corner enhancement," *IEEE Trans. Pattern Anal. Mach. Intell.*, vol. 14, no. 8, pp. 826–833, Aug. 1992.

[11] B. Fischl and E. L. Schwartz, "Adaptive nonlocal filtering: A fast alternative to anisotropic diffusion for image enhancement," *IEEE Trans. Pattern Anal. Mach. Intell.*, vol. 21, no. 1, pp. 42–48, Jan. 1999.

[12] S. H. Chang, L. Gong, M. Li, X. Hu, and J. Yan, "Small retinal vessel extraction using modified Canny edge detection," *Proc. IEEE*, vol. 96, no. 8, pp. 1255–1259, Aug. 2008.

[13] J. Li, J. Randall, and L. Guan, "Perceptual image processing for digital edge linking," in *Proc. IEEE Canadian Conf. Electr. Comput. Eng.*, Sep. 4, 2003, vol. 2, pp. 1215–1218.

[14] Z. Liping, L. Guangyao, and H. Zhu, "The generation algorithm of tissue contour lines in medical image," in *Proc. Int. Conf. Bioinformat. Biomed. Eng.*, 2008, pp. 2631–2634.

[15] T. Mondal, A. Jain, and H. K. Sardana, "Generation algorithm of craniofacial structure contour in cephalometric images," in *Proc. SPIE*, Feb. 2010, vol. 7546, p. 75460Z-10Z-10 .

[16] L. Lam, S. W. Lee, and C. W. Suen, "Thinning methodologies—A comprehensive survey," *IEEE Trans. Pattern Anal. Mach. Intell.*, vol. 14, no. 9, pp. 869–885, Sep. 1992.

Tanmoy Mondal received the B.Tech. degree in information technology from West Bengal University of Technology, Kolkata, India, in 2007, and the M.Tech. degree in mechatronics from Bengal Engineering and Science University, Kolkata, in 2009.

He was a Research Fellow with the Computational Instrumentation Unit, Central Scientific Instruments Organisation, Chandigarh, India, in 2008. In 2010, he joined Graphics and Inteligence Based Script Technology, Centre for Development of Advanced Computing, Pune, India. His research interests include pattern recognition, image processing and analysis, and computer vision. His current research is mainly related to exploiting camera-enabled mobile phones for optical character recognition of Indian languages.

Ashish Jain received the B.E. degree in electronics and instrumentation from the Institute of Technology and Management, Gwalior, India, in 2005, and the M.Tech. degree in biomedical engineering from Vellore Institute of Technology, Vellore, India, in 2007.

He then joined the Computational Instrumentation Unit, Central Scientific Instruments Organization, Chandigarh, India. His research interests include image processing and analysis, digital pathology, tele-imaging, and pattern recognition.

H. K. Sardana received the B.S. degree in electronics and communication engineering from Regional Engineering College (now NIT), Kurukshetra, India, the M.E. degree from Punjab Engineering College (now PEC University), Chandigarh, India, in 1989, and the Ph.D. degree from the University of Nottingham, Nottingham, U.K., in 1993.

He is currently a Scientist with the Central Scientific Instruments Organisation (CSIO), Chandigarh, India. He held a Nehru Centenary British Fellowship from 1990 to 1993 in the U.K. With the formation of the Academy of Scientific and Innovative Research (AcSIR), he is Coordinator and Professor for the M.Tech and Ph.D. programs being undertaken at CSIO, Chandigarh. He is also an Honorary Professor (Adjunct) with the Bengal Engineering and Science University, Shibpur, Kolkata, India for graduate studies in mechatronics. His interests include human computer interface, image processing, and pattern recognition. He has authored or coauthored more than 25 publications in research journals and conferences and holds four Patents. He is a reviewer for *Machine Vision and Applications* and *Defence Science Journal*.